NASA TECHNICAL NOTE

NASA TN D-2196

EFFECT OF WEIGHT, DENSITY, AND HEAT LOAD ON THERMAL-SHIELDING PERFORMANCE OF PHENOLIC NYLON

by Andrew J. Chapman

Langley Research Center
Langley Station, Hampton, Va.

NATIONAL AERONAUTICS AND SPACE ADMINISTRATION • WASHINGTON, D. C. • JUNE 1964

EFFECT OF WEIGHT, DENSITY, AND HEAT LOAD ON THERMAL-SHIELDING PERFORMANCE OF PHENOLIC NYLON

By Andrew J. Chapman

Langley Research Center
Langley Station, Hampton, Va.

NATIONAL AERONAUTICS AND SPACE ADMINISTRATION

For sale by the Office of Technical Services, Department of Commerce,
Washington, D.C. 20230 -- Price $0.75

EFFECT OF WEIGHT, DENSITY, AND HEAT LOAD ON THERMAL-SHIELDING PERFORMANCE OF PHENOLIC NYLON

By Andrew J. Chapman

SUMMARY

Phenolic-nylon heat-shield specimens of identical configuration have been tested at varying unit weight, density, and total heat load in an electric-arc-heated airstream. The stream stagnation enthalpy was approximately 3,000 Btu/lb, and the heating rate to the specimens was between 90 and 120 Btu/ft^2-sec. The results of these tests indicate that low-density phenolic nylon experienced a lower rate of mass loss and temperature penetration on a unit-weight basis than did high-density phenolic nylon. The mass loss or pyrolysis rate approached a quasi-steady value with increasing heat load. A thermal-shielding efficiency, defined as the quotient of the total heat load and the unit weight of material, was increased primarily by reducing the density of the material. Efficiency was also increased by allowing the maximum back-surface-temperature rise to increase.

INTRODUCTION

The requirement for a thermal-shielding system which can provide efficient protection for manned vehicles entering a planetary atmosphere at escape velocity has led to the development of materials which will simultaneously dissipate heat by thermal degradation and reradiation. A comparative investigation (ref. 1) indicates that a class of such materials, which are known as charring ablators, are among the more effective thermal-protection systems. Other investigations have studied the effects of heating rate (refs. 2, 3, and 4), atmospheric composition (refs. 3 and 5), and material composition (ref. 6) on materials of this type.

In the present investigation a typical charring composite material was tested in an electric-arc-heated airstream to study the effect of varying total heat load, unit weight, and density on thermal-shielding performance. The material was a molded combination of phenolic resin and nylon powder which has been widely investigated and used as a reference material for comparing the performance of other charring-composite materials (refs. 1 to 6).

SYMBOLS

c_p	specific heat at constant pressure, Btu/lb-^{o}R
E	thermal shielding efficiency Q/w, Btu/lb
k	thermal conductivity, Btu/ft-sec-^{o}R
Q	total front-surface cold-wall heat load, Btu/ft^2
Q_B	total heat transferred to back surface of material specimen, Btu/ft^2
q	average cold-wall heat-transfer rate for exposure period in test stream, Btu/ft^2-sec
T	temperature, ^{o}F
ΔT	back-surface-sensor-temperature rise, ^{o}F
$(dT/dt)_f$	maximum rate of temperature rise at termination of exposure, ^{o}F/sec
t	time, sec
w	material specimen unit weight, lb/ft^2
ρ	density, lb/ft^3
τ	thickness of metal calorimeter, ft

Subscripts:

o	initial value
cu	properties of copper
f	value at end of exposure in test stream
m	maximum

TEST FACILITY

The 2,500-kilowatt arc-powered jet at the Langley Research Center was used for this investigation. The arc jet is shown in figure 1 with the inserter mechanism which positioned the material specimen and heating-rate probe in the test stream. Characteristics of the test stream for the present investigation are given in table I. A more complete description of the facility is given in reference 1.

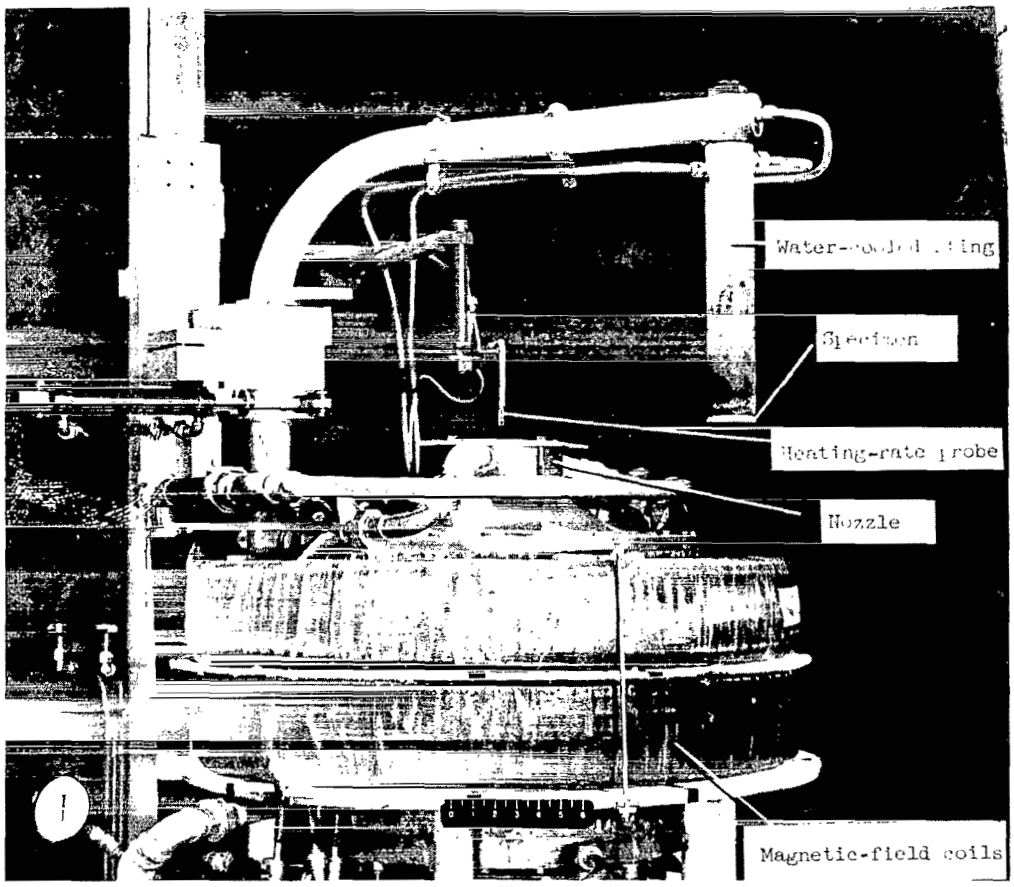

L-61-3423.1

Figure 1.- The 2,500-kilowatt arc-powered jet at the Langley Research Center.

TEST MATERIAL AND SPECIMEN ASSEMBLY

Phenolic Nylon

The material investigated was a molded composition of phenolic resin and nylon powder containing 50 percent by weight of each component. Density of the material was varied in some specimens by replacing one-half of the phenolic resin with phenolic Microballoons. This type of phenolic nylon was also investigated in reference 1. The composition and nominal density of these materials are given in table II.

Specimen Configuration and Instrumentation

The material specimens were flat discs having a diameter of 3 inches and a thickness determined by the density (table II) and unit weight. The specimen

unit weights were 1.5, 3.0, and 6.0 lb/ft^2. Photographs of several specimens before testing are shown in figure 2.

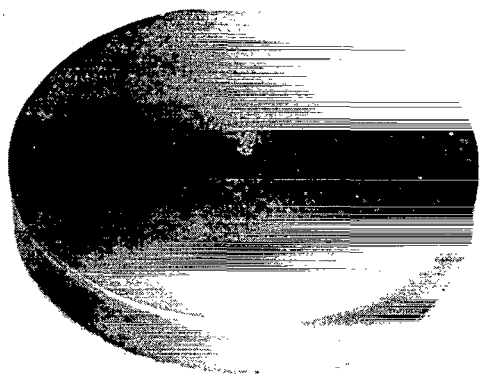

(a) High-density phenolic nylon. L-63-5660

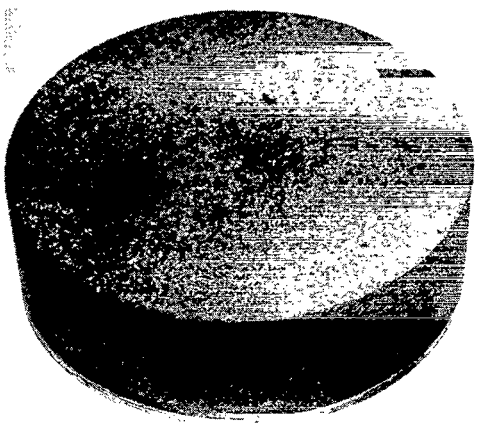

(b) Low-density phenolic nylon. L-63-5659

Figure 2.- Phenolic nylon before exposure in test stream.

The specimen assembly consisted of the material specimen with a brass mounting ring and a copper sensor bonded to the back surface as shown in figure 3. The back-surface sensor consisted of a 0.125-inch-thick copper disc and concentric guard ring with thermocouples attached in the positions shown in figure 3. Heat transfer through the specimen was indicated by the temperature and heat capacity of the center disc, which acted as a calorimeter. The sensor side of the specimen was mounted in a water-cooled sting as shown in figure 3.

TEST PROCEDURE

The arc jet was operated for several seconds before beginning a test to allow stream conditions to stabilize. A heating-rate probe was then positioned in the stream for a short period of time and the heating rate was recorded oscillographically. After removing the heating-rate probe, the material specimen was positioned in the test stream. Temperature-rise values on the back-surface sensor were recorded throughout exposure, and the specimen was removed from the stream when predetermined temperature-rise values (50° F or 300° F) occurred on the back-surface calorimeter. After the specimen was removed, the heating-rate probe was repositioned in the stream for several seconds and the jet was then stopped. After exposure the temperatures on the back-surface sensor were recorded until a maximum temperature rise on the calorimeter was indicated.

Heating-Rate Measurements

The heating rate for a 3-inch-diameter flat material specimen was determined by calibrated measurements of heating rate obtained with a 3/8-inch-diameter continuous-reading water-cooled probe. The method and the probe are described in reference 1.

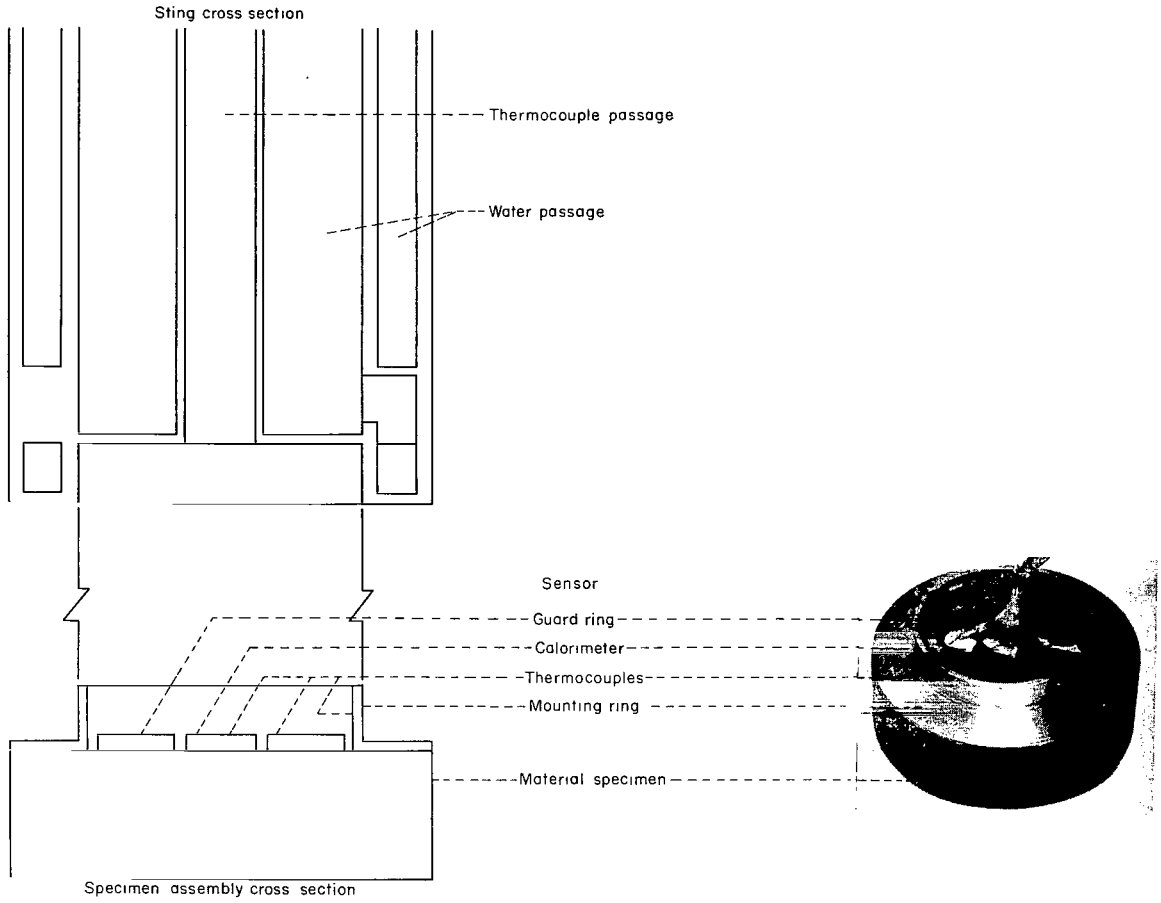

Figure 3.- Material specimen instrumentation and mounting detail. L-64-351

Test Stream Calibration

Static temperature of the test stream was measured by the spectrographic method described in reference 1. Free-stream enthalpy was determined from the static temperature at a pressure of 1 atmosphere (see table I) by using a Mollier diagram for air in chemical equilibrium. Stagnation enthalpy was approximately equal to free-stream enthalpy since only a small part of the total stream energy was derived from the velocity of the stream.

RESULTS

The test stream conditions were held approximately constant for all tests (table I). The density and unit weight of the materials were varied as described in the section entitled "Test Materials and Specimen Assembly," and the exposure

period and total heat load were varied by terminating exposure at back-surface-temperature-rise values of 50° F or 300° F. Test results were obtained in the form of back-surface-temperature time histories and thickness of the residual specimen material. The results for each test are given in table III. The back-surface-temperature histories are described by the time at which the back-surface calorimeter experienced a temperature rise of 50° F or 300° F (for long exposure periods), total exposure time, temperature rise at termination of exposure, temperature-rise rate at termination of exposure, and the maximum temperature rise with the time at which it occurred. The thickness of the residual material was equal to the char-layer thickness plus the thickness of the sublayer of virgin material when it existed. Also presented are the total back-surface heat load, average cold-wall heating rate to the front surface of the specimen and the total cold-wall heat load to the front surface.

Tests of 6 lb/ft^2 low-density phenolic-nylon specimens, which were very thick, resulted in uneven reduction in diameter, or undercutting, near the back-surface bond line. Because of this uneven ablation, the effects of two-dimensional heat transfer in the plane of the back surface were greatly exaggerated and the results were not comparable with those of other tests. For this reason, results for the 6 lb/ft^2 low-density phenolic-nylon specimens are not presented.

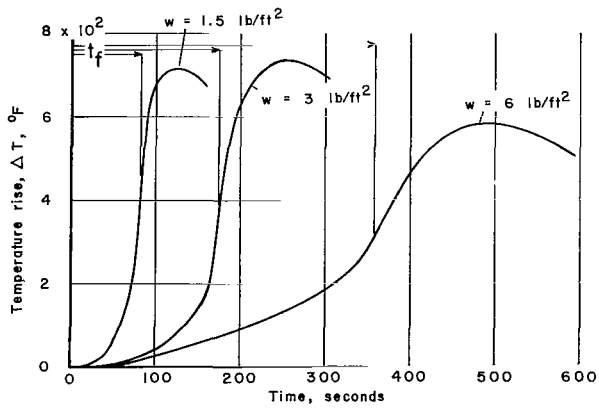

(a) Long exposure period $\Delta T_f \approx 300^\circ$ F.

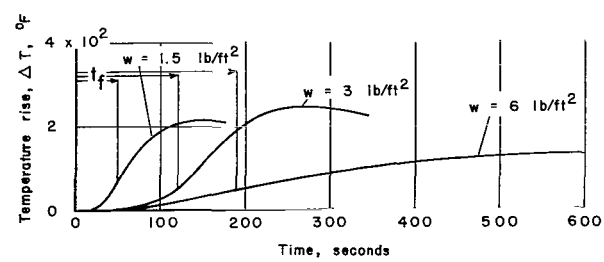

(b) Short exposure period $\Delta T_f \approx 50^\circ$ F.

Figure 4.- Typical back-surface-temperature histories for varying unit weight and exposure period: high-density phenolic nylon.

Back-Surface-Temperature Histories

Typical back-surface-temperature histories for each unit weight and exposure period are shown in figure 4 for high-density phenolic nylon and in figure 5 for low-density phenolic nylon. These figures show that the temperature-rise rate was quite low at the beginning of exposure, but accelerated near termination of exposure, and reached a maximum rate at termination. This maximum temperature-rise rate was considerably greater at the termination of the long exposure periods than at the termination of the short exposure periods; this greater temperature-rise rate was the result of the original material being completely pyrolized in the long exposure period leaving only a residual layer of char over the sensor, while a layer of unpyrolized material which acted as insulation was adjacent to the sensor after the short exposure period. In

all cases the temperature rise continued after termination of exposure and the maximum temperature which occurred in the postexposure period determined the total quantity of heat transferred through the specimen.

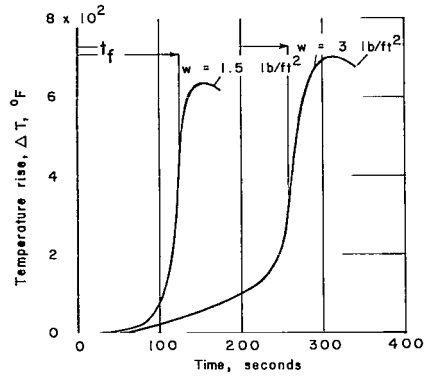

(a) Long exposure period $\Delta T_f \approx 300^\circ$ F.

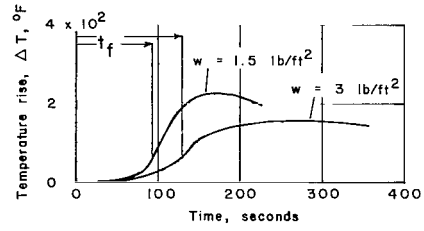

(b) Short exposure period $\Delta T_f \approx 50^\circ$ F.

Figure 5.- Typical back-surface-temperature histories for varying unit weight and exposure period: low-density phenolic nylon.

Appearance of Exposed Material

High-density phenolic nylon.- The long exposure periods which terminated at a back-surface-temperature rise of approximately 300° F resulted in all the original material being affected by pyrolysis. A layer of low-density char was formed which had a columnar structure oriented with the thickness (fig. 6(a)). This char layer comprised the entire residual material from the 1.5 lb/ft^2 and 3 lb/ft^2 specimens. In addition to the outer char layer, the material remaining from the 6 lb/ft^2 specimen had a sublayer of partially decomposed material adjacent to the back-surface sensor. This sublayer was more dense than the completely charred layer and the columnar structure was not evident.

The short exposure period which terminated at a 50° F back-surface-temperature rise (fig. 6(b)) did not produce complete pyrolysis of the original material. All specimens had an outer layer of completely charred material which separated from a sublayer of incompletely charred material and virgin material. The outer char layer was identical to that from the tests at long exposure periods, while the inner layer had a thin coating of less developed char integral with the residual virgin material. This indicated a gradient of char development or pyrolysis between the completely charred material and the virgin material.

The gradient of char development is described in reference 5 and is shown in figure 7. Five zones of thermal degradation are shown. The carbonaceous char layer is completely degraded material. Separation of the char layer occurred at the zone of phenolic decomposition as the specimen cooled after exposure. The remaining three zones of partial degradation comprise the coating of less developed char which was integral with the virgin material. In the present discussion, however, the char-virgin-material interface is considered to be the zone of phenolic decomposition or separation.

Low-density phenolic nylon.- The long exposure periods resulted in complete pyrolysis of the original material as was the case for high-density phenolic nylon. A thin layer of char remained over the sensor although the mounting ring

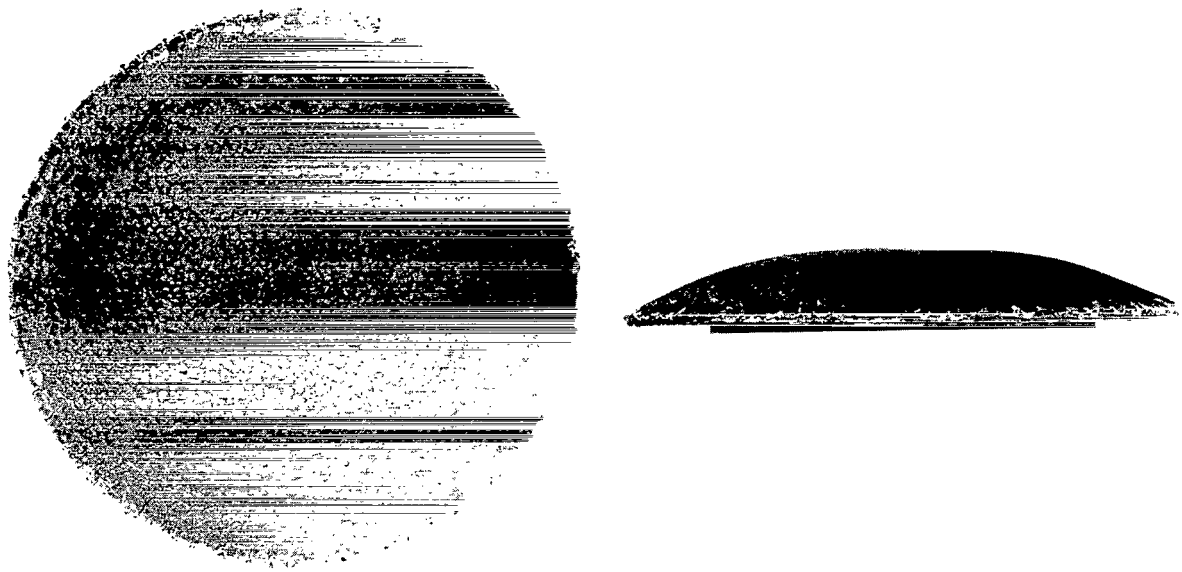

(a) Exposure terminated at 300° F back-surface-temperature rise.

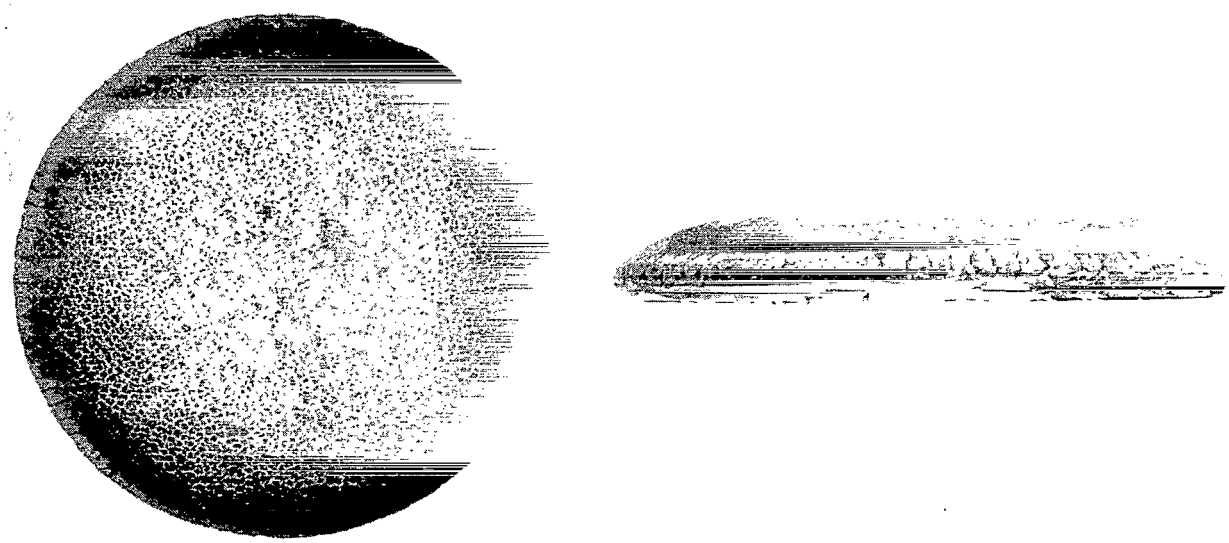

(b) Exposure terminated at 50° F back-surface-temperature rise. L-64-365

Figure 6.- High-density phenolic nylon after exposure.

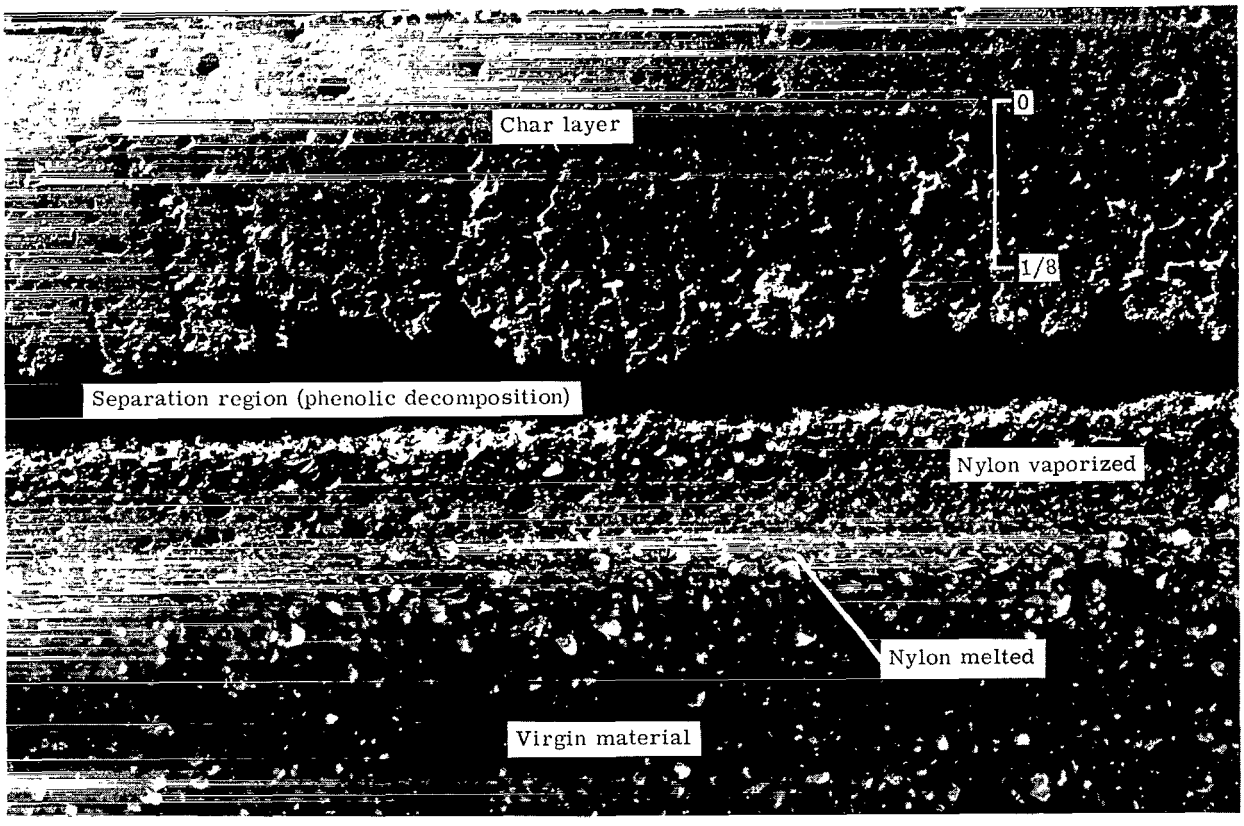

Figure 7.- Identification of thermal degradation zones. L-64-354

was exposed in several places (fig. 8(a)). The char had approximately the same structure as that from the high-density phenolic nylon.

The short exposure periods resulted in incomplete pyrolysis of the original low-density specimens as was the case for the high-density material (fig. 8(b)). However, the outer char layer did not separate easily from the sublayer of virgin material as it did for the high-density phenolic nylon. The char layer and sublayer of virgin material and partially decomposed material were similar in appearance to the residual high-density material.

DISCUSSION

Mass Transfer and Temperature Penetration

The material which remained after exposing the specimens in the test stream consisted of a layer of completely charred material and, in some cases, a sublayer of incompletely charred material and virgin material. The appearance of the residual material was described in the previous section. The thickness of

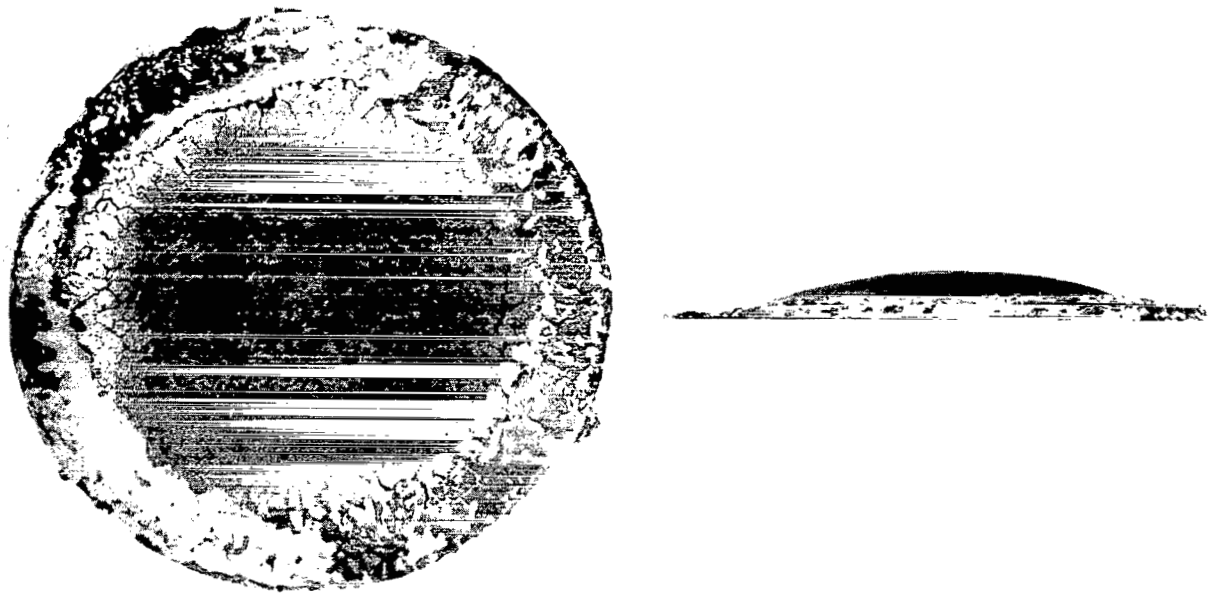

(a) Exposure terminated at 300° F back-surface-temperature rise.

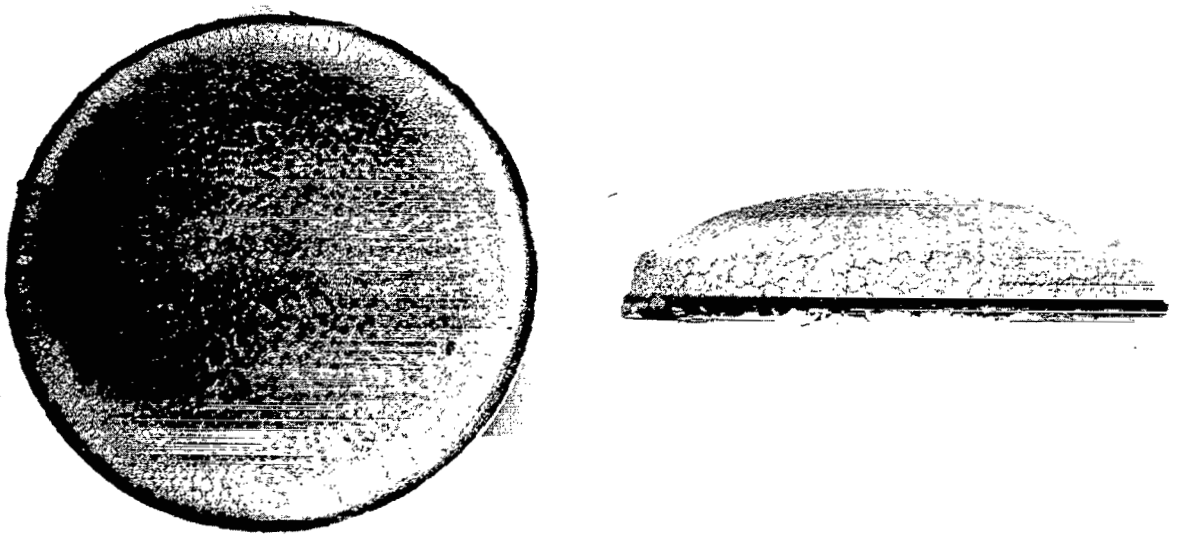

(b) Exposure terminated at 50° F back-surface-temperature rise. L-64-366

Figure 8.- Low-density phenolic nylon after exposure.

these layers for each test is given in table III(a) for high-density phenolic nylon and in table III(b) for low-density phenolic nylon. In figure 9 the positions of the char layers and sublayers relative to original specimen thickness are shown as a function of exposure time. These plots of individual test points represent composite time histories of the recession of the pyrolysis interface and the char surface.

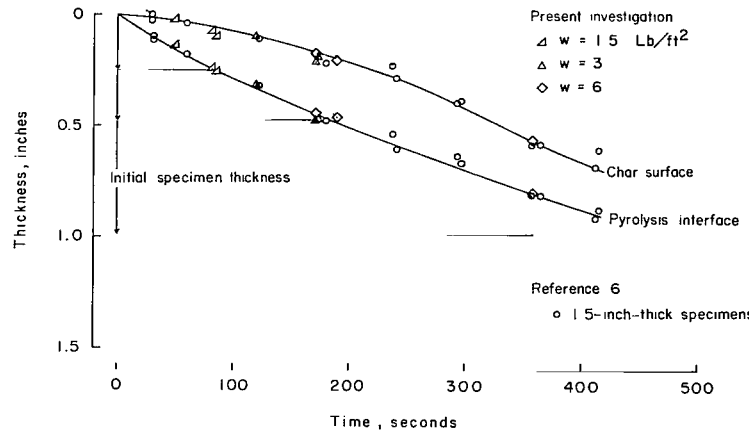

(a) High-density phenolic nylon.

Figure 9.- Char-surface recession and pyrolysis-interface-recession time history during exposure in test stream.

Data from reference 6 are also shown in figure 9. These were obtained from vertically sectioned 1.5-inch-thick phenolic-nylon specimens which had been exposed at periods of progressing length in a test environment identical to that of the present investigation. The present data agree very well with that of reference 6 even though the specimens used in reference 6 were 1.5 to 6 times as thick as those of the present tests.

Char-surface and pyrolysis-interface recession.- Figure 9(a) shows that the char-surface-recession rate of high-density phenolic nylon increased during approximately the first 300 seconds of exposure time after which it decreased slightly and approached a constant value. The recession rate of the pyrolysis interface decreased from the initial value and appeared to approach a constant value after about a 300-second exposure.

In figure 9(b) it may be seen that the char-surface regression rate of low-density phenolic nylon accelerated rapidly during the first 100 seconds of exposure after which it decreased and appeared to approach a constant value. The recession rate of the interface decreased slightly during the first 100 seconds of exposure and then appeared to approach a constant value. The char-surface and pyrolysis-interface recession rates were considerably greater for low-density phenolic nylon than for high-density phenolic nylon. Also the

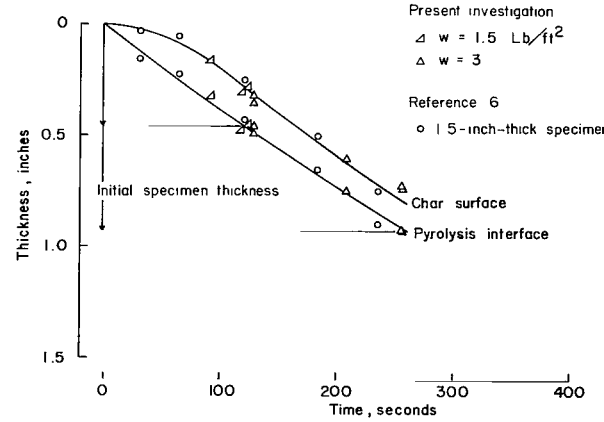

(b) Low-density phenolic nylon.

Figure 9.- Concluded.

char layer was thinner for low-density phenolic nylon than it was for high-density phenolic nylon.

Temperature penetration.- In figure 10 exposure times for 300° F and 50° F back-surface-temperature-rise values have been plotted against original specimen thickness. Curves fitted to these points represent composite time histories for penetration of isotherms into the phenolic nylon. Isotherms obtained from reference 6 are also shown in figure 10. These data were obtained from 1.5-inch-thick specimens with thermocouples spaced at varying depths within the material. The char-surface and pyrolysis-interface position-time curves from figure 9 are also shown in figure 10.

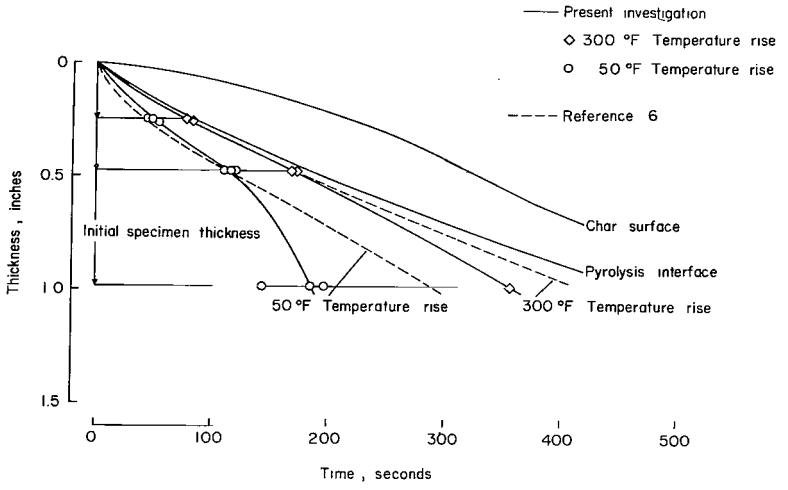

(a) High-density phenolic nylon.

Figure 10.- Temperature-penetration, pyrolysis-interface-recession, and char-surface-recession time history during exposure in test stream.

The temperature-penetration data for high-density phenolic nylon in figure 10(a) show that the 300° F isotherm remained close to the pyrolysis interface and had about the same rate of penetration during the first 180 seconds of exposure. Agreement with the 300° F isotherm of reference 6 was close during this period. After a 180-second exposure, the 300° F isotherm had a slightly increasing rate of penetration while the penetration rate of the pyrolysis interface approached a constant value. The penetration rate of the 300° F isotherm was also greater than that for reference 6 after a 180-second exposure. The 50° F isotherm appeared to have only a slightly greater rate of penetration than the pyrolysis interface at 100 seconds of exposure; however, after this time the rate of penetration increased very rapidly. Agreement with the 50° F isotherm of reference 6 was good up to 100 seconds of exposure but the data from reference 6 indicated only a slight increase in penetration rate after that time.

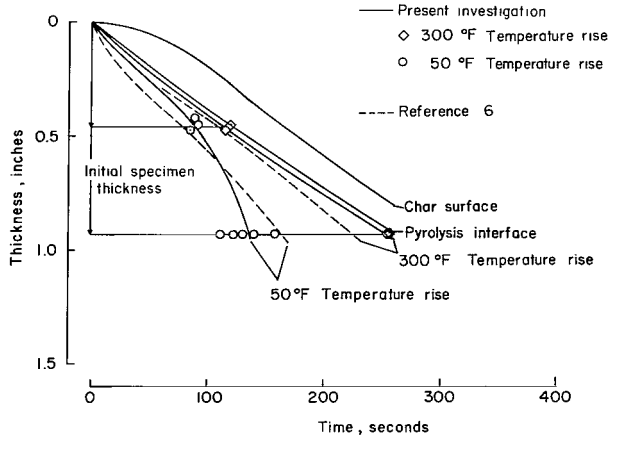

(b) Low-density phenolic nylon.

Figure 10.- Concluded.

Temperature-penetration data for low-density phenolic nylon in figure 10(b) show that the 300° F isotherm remained very close to the pyrolysis interface and had about the same rate of penetration throughout the exposure period. The 50° F isotherm had a moderate rate of penetration during the first 90 seconds of exposure time. After that time the rate of penetration increased rapidly. However, there was some uncertainty as to the position of the 50° F isotherm at extended exposure time because of the scatter of the data for thick low-density specimens. Figure 10 shows that the rate of temperature penetration relative to thickness was greater for low-density phenolic nylon than it was for high-density phenolic nylon.

Effect of unit weight and density.- It has been shown that low-density phenolic nylon experienced a higher rate of char surface and interface recession and a higher rate of temperature penetration based on thickness than high-density phenolic nylon. However, it is usually more important to consider the performance of thermal-shielding materials on a basis of weight rather than thickness. The interface-position and temperature-penetration curves in figure 10 are plotted in figure 11 as a function of material unit weight. This has

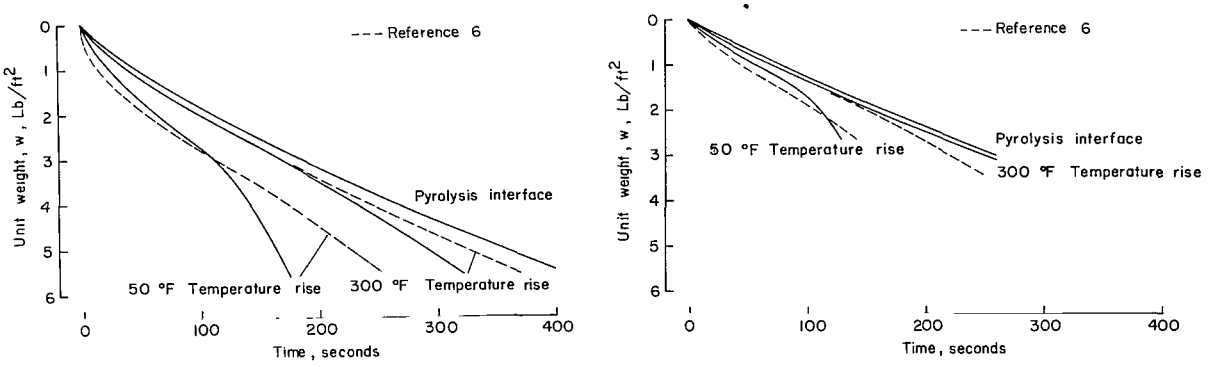

(a) High-density phenolic nylon.

(b) Low-density phenolic nylon.

Figure 11.- Mass-transfer and temperature-penetration time history during exposure in test stream.

been accomplished by multiplying thickness by the nominal density of the material given in table II. Figure 11 shows that low-density phenolic nylon experienced a lower rate of pyrolysis and temperature penetration based on unit weight than did high-density phenolic nylon.

The rate of pyrolysis for both materials appeared to approach a quasi-steady value. The rate of temperature penetration appeared to approach a quasi-steady value during the initial part of the exposure period. The subsequent increase in the rate of temperature penetration was the result of lateral heating. This was particularly noticeable in thicker specimens at lower values of temperature rise and exposure time.

Total Back-Surface Heat Load and Thermal-Shielding Efficiency

The mass-transfer and temperature-penetration effects discussed in the previous section all occurred while the specimens were being exposed in the test stream. However, as indicated previously, the temperature at the back surface of the specimen continued to rise after termination of exposure (see figs. 4 and 5), and the maximum temperature rise at the back-surface calorimeter was an indication of the total quantity of heat which reached the back surface. Thermal-shielding performance of the phenolic-nylon materials may be further evaluated in terms of this total back-surface heat load Q_B. The measured variable quantities which affected this parameter were the unit weight of the shield material, the density of the material, and the exposure time or total heat load.

The total back-surface heat load was determined from the maximum back-surface-temperature rise and the heat capacity of the calorimeter in the following manner:

$$Q_B = \left(c_p \rho \tau\right)_{cu} \Delta T_m \tag{1}$$

The heat capacity of the copper calorimeter was $\left(c_p \rho \tau\right)_{cu} = 0.544$ Btu/ft^2-$^\circ$F.

The heating rate to the front surface of the specimen was determined by measurements made immediately before and after exposure of the specimen in the test stream (see section entitled "Test Procedure"). The cold-wall heating rate q was an average value of these measurements. Heating-rate values for each test are shown in table III. During all tests there was a negligible variation of heating rate over the period of specimen exposure. The measured heating-rate values for the test series varied from 90 to 120 Btu/ft^2-sec. Total cold-wall heat load to the front surface of the specimen was determined in the following manner:

$$Q = t_f q \tag{2}$$

The total back-surface heat load and the other quantities varied in these tests may be correlated by dimensional analysis. There are seven quantities which may be considered. These quantities may be expressed in terms of five units, and therefore will form two independent dimensionless products:

$$\frac{Q_B}{Q} \quad \text{and} \quad \left(\frac{t}{w^2} \frac{\rho k}{c_p}\right)$$

The known values in each of these products may be plotted to show their relation. In figure 12 experimental values of Q_B/Q are shown as a function

of $\frac{\sqrt{t_f}}{w}$. The curves fitted to these points represent equations of the form:

$$\frac{Q_B}{Q} = \text{Constant} \left(\frac{t}{w^2} \frac{\rho k}{c_p} \right)^{\text{Constant}} \qquad (3)$$

If all of the material properties ρ, k, and c_p were accurately known for the two types of phenolic nylon, these could be inserted into equation (3) and the constant coefficient and exponent could be determined experimentally. In the present tests only the density ρ of the materials is known so that the mass thermal diffusivity $\rho k/c_p$ is included in the constant coefficient term. It may be noted, however, that the fraction of the total cold-wall heat load transferred to the shield back surface would increase with increasing values of $\rho k/c_p$.

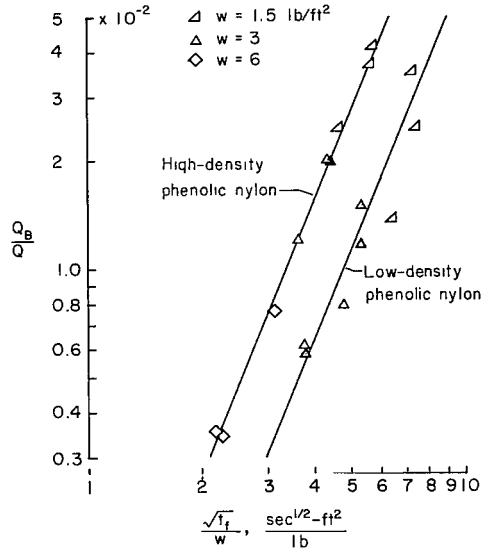

Figure 12.- Fraction of total cold-wall heat load transferred to back surface of material specimen as a function of exposure time and unit weight.

Emperical relations of the same form as equation (3) have been obtained from the experimental data in figure 12. The relation for high-density phenolic nylon is

$$\frac{Q_B}{Q} = 4.50 \times 10^{-4} \left(\frac{\sqrt{t_f}}{w} \right)^{2.55} \qquad (4a)$$

and the relation for low-density phenolic nylon is

$$\frac{Q_B}{Q} = 1.84 \times 10^{-4} \left(\frac{\sqrt{t_f}}{w} \right)^{2.55} \qquad (4b)$$

These relations fit the experimental data very well; however, there was some scatter for the low-density phenolic-nylon data. It must be realized that these equations apply only for phenolic nylon in the present test environment.

It is shown in figure 12 that the fraction of the total cold-wall heat load which reached the back surface of the shield specimen increased with increasing exposure time and decreased with increasing unit weight. It is also shown that, for given values of exposure time and unit weight, this heat-load fraction was lower for low-density phenolic nylon than it was for high-density phenolic nylon.

A thermal-shielding efficiency, or effective heat capacity, may be defined as the quotient of the total cold-wall heat load and a unit weight of material. In previous investigations (refs. 1, 2, and 3) this parameter was referenced to a constant back-surface-temperature rise at the termination of heating. However, in the present tests the shielding efficiency is partially evaluated in terms of varying back-surface-temperature rise. Also, the back-surface temperature used is the maximum value which occurred after termination of exposure rather than the value at the termination of exposure. The temperature at the termination of exposure represented a transient condition, while the maximum back-surface temperature was a final result of the heating conditions encountered by the specimen.

An expression for shielding efficiency may be obtained by rearranging equations (4) and inserting equations (1) and (2). The expression for high-density phenolic nylon is

$$E = \frac{Q}{w} = 22.70(\Delta T_m)^{0.44} q^{0.56} w^{0.12} \tag{5a}$$

and the corresponding expression for low-density phenolic nylon is

$$E = \frac{Q}{w} = 33.65(\Delta T_m)^{0.44} q^{0.56} w^{0.12} \tag{5b}$$

Maximum back-surface-temperature rise has been used in place of total back-surface heat load to provide a more conventional indication of performance.

Elimination of exposure time by substituting equation (2) in equations (4) suggests that shielding efficiency will increase with increasing heating rate. The range of heating rate in this investigation was too small to actually establish such a trend. However, it has been shown in reference 2 that the shielding efficiency of high-density phenolic nylon will increase with both convective and radiative heating rate as a result of higher char-surface temperature and consequently greater radiation from the surface.

Shielding efficiency is shown in figure 13 as a function of maximum back-surface-temperature rise for the values of unit weight used in the tests. These curves were calculated from equations (5) by using a heating rate of 105 Btu/ft^2-sec which represented an average of the values measured during the tests. The experimental points in figure 13 were also corrected for this heating rate. The high-density phenolic-nylon data in figure 13(a) fall close to the curves for corresponding unit weight. There is some scatter for the low-density phenolic-nylon data in figure 13(b); however, these data do follow the trend of increasing efficiency with increasing back-surface-temperature rise. The scatter of the data for low-density phenolic nylon which is evident in figures 12 and 13 was probably the result of a slight variation in composition or molding procedure. Figure 13 shows that shielding efficiency was primarily affected by changing the density or the maximum back-surface-temperature rise and was affected to a very small extent by changing the unit weight.

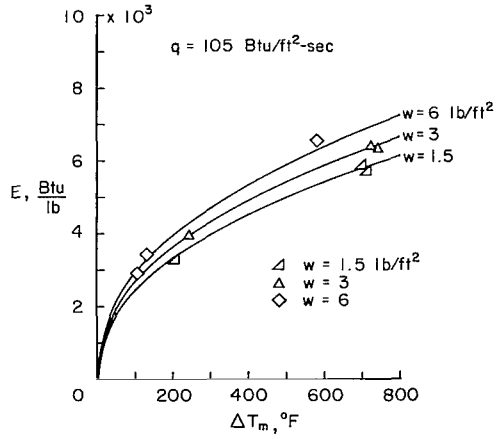

(a) High-density phenolic nylon.

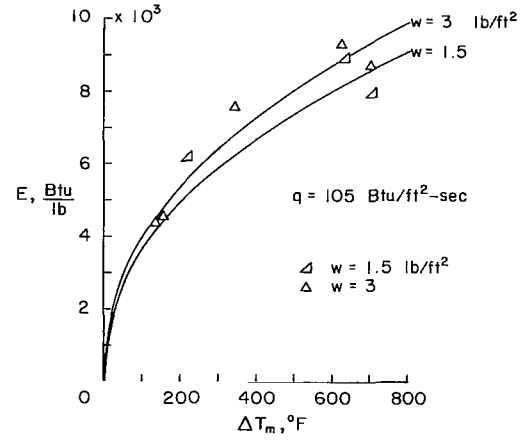

(b) Low-density phenolic nylon.

Figure 13.- Thermal-shielding efficiency as a function of maximum back-surface-temperature rise and unit weight.

The increase in thermal-shielding efficiency which could be gained by varying the other experimental parameters is shown in figure 14. These curves were obtained from equations (5) and are expressed as ratios to an initial value of the quantities in question. The change predicted by varying one parameter was obtained while holding constant the quantities not being considered. It is shown that approximately a 49-percent increase in efficiency was obtained by reducing the density by a factor of 0.52. An increase in efficiency was also obtained by allowing the maximum back-surface-temperature rise to increase. However, it was necessary to allow the maximum back-surface temperature to increase by a factor of approximately 2.5 to achieve the same increase in efficiency which was obtained by reducing the density by a factor of 0.52. There was, of course, a limit to which the back-surface temperature could be increased to obtain an increase in efficiency since the specimens were completely reduced to char when the back-surface temperature rose 700° F. It is also shown that a slight gain in efficiency was obtained when the unit weight was increased. This means that if the total heat load were increased, the unit weight would

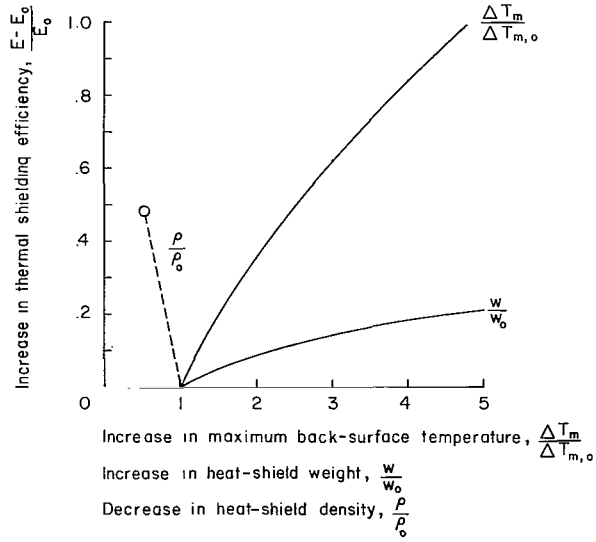

Figure 14.- Increase of thermal-shielding efficiency for phenolic nylon.

not have to be increased by the same amount to limit the back-surface temperature to a given value.

The heat-shield weight required to limit the maximum back-surface-temperature rise may be obtained by rearranging equation (4) and substituting equations (1) and (2). The expression for high-density phenolic nylon is

$$w = 0.0617 \frac{Q^{0.892}}{q^{1/2}(\Delta T_m)^{0.392}} \tag{6a}$$

and the expression for low-density phenolic nylon is

$$w = 0.0435 \frac{Q^{0.892}}{q^{1/2}(\Delta T_m)^{0.392}} \tag{6b}$$

Heat-shield unit weight is shown in figure 15 as a function of maximum back-surface-temperature rise for values of cold-wall heat input. These curves were

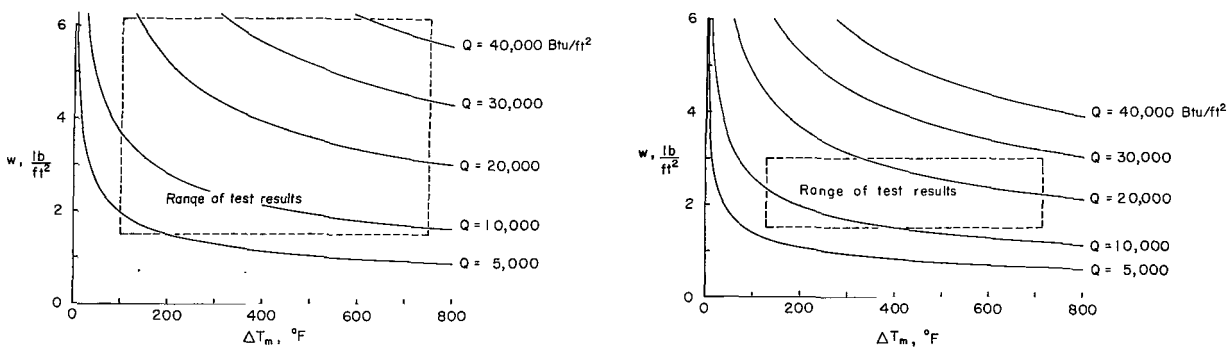

(a) High-density phenolic nylon.

(b) Low-density phenolic nylon.

Figure 15.- Heat-shield weight required for maximum back-surface-temperature rise and total heat load.

calculated using a heating rate of $q = 105$ Btu/ft^2-sec. The areas enclosed by the dashed lines approximately represent the range covered in the present tests. It is obvious from equations (6) and figure 15 that a lower heat-shield weight is required for a given heat load if the maximum back-surface-temperature rise is allowed to increase. It is also shown that for a given heat load a lower weight of low-density phenolic nylon is required to limit the back-surface temperature to a given maximum value than is required for high-density phenolic nylon. It is suggested by equations (6) that, for a given heat load and back-surface-temperature rise, heat-shield weight could be reduced by increasing the heating rate. This, however, was not demonstrated in the investigation..

The extent to which heat-shield weight was reduced by varying other parameters is shown in figure 16. These curves were obtained from equations (6) in the same manner that the curves in figure 14 were obtained from equations (5). It is shown that reducing the density by a factor of 0.52 would permit approximately a 30-percent reduction of heat-shield weight with heat load and back-surface-temperature rise held constant. It would be necessary to reduce the total heat load by a factor of approximately 0.7 or to allow the maximum back-surface temperature to increase by a factor of approximately 2.5 to obtain the same reduction of weight.

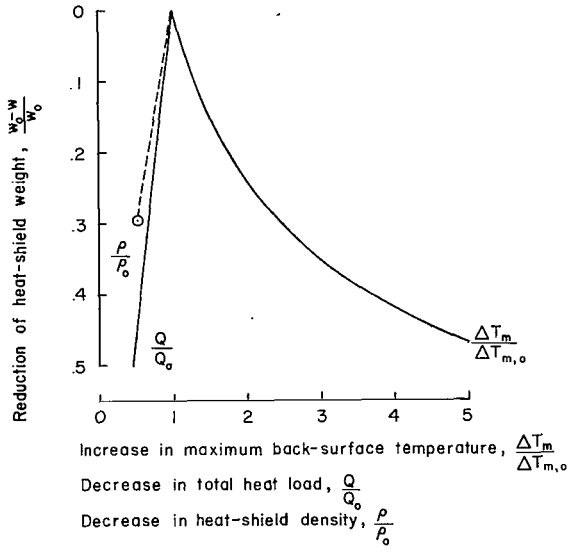

Figure 16.- Reduction of heat-shield weight for phenolic nylon.

Comments on the Experimental Method

Effect of lateral heating.- The specimen assembly and water-cooled sting were designed to minimize the effects of lateral or two-dimensional heating on the temperature indicated at the back-surface calorimeter. However, the temperatures monitored on the specimen mounting ring and back-surface sensor components indicate a temperature gradient in the back-surface plane. The positions where these temperatures were measured are shown in figure 3. Temperature histories on the mounting ring, guard ring, and calorimeter for a typical test are shown in figure 17. The temperature of the mounting ring increased at the beginning of exposure and maintained a higher value than that of the guard ring or calorimeter until near the end of exposure. The temperature of the mounting ring was maintained at an approximately constant value by the water flow in the sting. The temperature history of the guard ring was similar to that of the calorimeter but was slightly higher throughout the test.

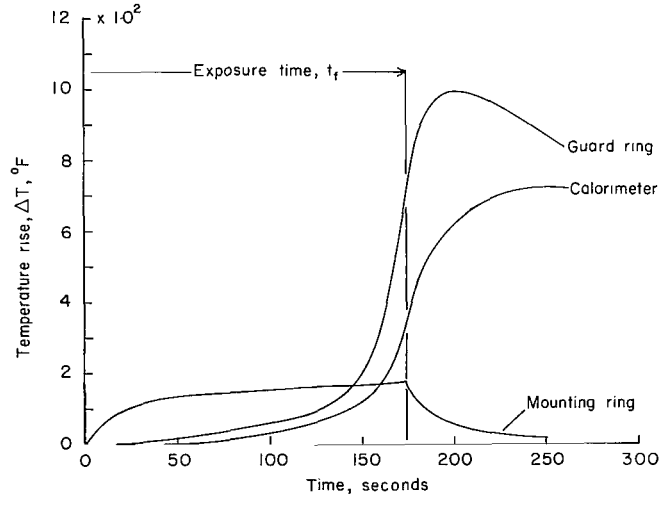

Figure 17.- Back-surface assembly temperature histories for a typical test.

The effect of lateral heating may be seen in the rapidly increasing rate of penetration of the 50° F isotherms in figure 10. The more rapid rate occurred because the difference in lateral heat transfer and heat transfer in the longitudinal direction was less for the

thicker specimens at short exposure time than it was for thinner specimens or at longer exposure time after an appreciable amount of material had been ablated.

Analysis of experimental results.- The purpose of the analysis in the preceding section was to organize the test results and to show the trend of performance caused by varying each experimental parameter. However, it should be realized that the results of this analysis may be influenced by the configuration of the specimens and the test arrangement as well as by the reaction of the material. Therefore, great care should be taken when comparing the present test results with the results of other investigations where a different experimental method was used. The equations and numerical values obtained should be considered to apply only for the present test environment and arrangement unless further tests show that they are valid for a broader range of conditions.

CONCLUDING REMARKS

The thermal-shielding performance of phenolic-nylon specimens of identical configuration was evaluated at varying density, unit weight, and total heat load in an electric-arc-heated airstream. The stream stagnation enthalpy was approximately 3,000 Btu/lb and heating rates to the specimens were between 90 and 120 Btu/ft^2-sec.

At increasing total heat load in the test stream the low-density phenolic nylon experienced a lower rate of mass loss and a lower rate of temperature penetration based on unit weight than did the high-density phenolic nylon. However, the actual thickness of low-density phenolic nylon which was pyrolyzed was greater and the char-layer thickness was less than that of the high-density phenolic nylon. For both high- and low-density material, the pyrolysis and char-surface ablation rates approached quasi-steady values with increasing heat load. The rates of char-layer and pyrolysis-interface recession were not affected by the initial unit weight of the specimen.

A thermal-shielding efficiency, defined as the quotient of the total heat load and the unit weight of material, was increased primarily by reducing the density of the material. Shielding efficiency was increased approximately 49 percent when the density was reduced by a factor of 0.52. Shielding efficiency was also increased when the maximum back-surface temperature was allowed to increase. However, it was necessary to allow the maximum back-surface temperature to increase by a factor of 2.5 to obtain a 49-percent increase in efficiency.

Langley Research Center,
National Aeronautics and Space Administration,
Langley Station, Hampton, Va., November 27, 1963.

REFERENCES

1. Chapman, Andrew J.: An Experimental Evaluation of Three Types of Thermal Protection Materials at Moderate Heating Rates and High Total Heat Loads. NASA TN D-1814, 1963.

2. Peters, Roger W., and Wilson, R. Gale: Experimental Investigation of the Effect of Convective and Radiative Heat Loads on the Performance of Subliming and Charring Ablators. NASA TN D-1355, 1962.

3. Brooks, William A., Jr., Wadlin, Kenneth L., Swann, Robert T., and Peters, Roger W.: An Evaluation of Thermal Protection for Apollo. NASA TM X-613, 1961.

4. Swann, Robert T., and Pittman, Claud M.: Numerical Analysis of the Transient Response of Advanced Thermal Protection Systems for Atmospheric Entry. NASA TN D-1370, 1962.

5. Dow, Marvin B., and Swann, Robert T.: Determination of the Effects of Oxidation on the Performance of Charring Ablators. NASA TR R-196, 1964.

6. Peters, Roger W., and Wadlin, Kenneth L.: The Effect of Resin Composition and Fillers on the Performance of a Molded Charring Ablator. NASA TN D-2024, 1963.

TABLE I.- OPERATING CHARACTERISTICS OF 2,500-KILOWATT ARC-POWERED JET AT THE LANGLEY RESEARCH CENTER

Stream diameter, in.	4
Test medium	Air
Arc power (3-phase a-c), kw	1,560
Mass flow, lb/sec	0.35
Velocity, ft/sec	890
Mach number	0.21
Static enthalpy*, Btu/lb	3,000
Static pressure*, atm	1
Static temperature*, $^{\circ}R$	7,200
Heat-transfer rate to 3-inch-diameter flat surface, Btu/ft^2-sec	90 to 120
Maximum operating time	Continuous

*Approximate stagnation.

TABLE II.- COMPOSITION AND DENSITY OF PHENOLIC NYLON

Identification	Composition, percent by weight,			Density, ρ, lb/ft^3
	Phenolic resin	Phenolic Micro-balloons	Nylon powder	
High-density phenolic nylon	50		50	75
Low-density phenolic nylon	25	25	50	39

TABLE III.- SUMMARY OF TEST RESULTS

(a) High-density phenolic nylon

Original specimen		Specimen after exposure		Back-surface-temperature history							Heating rate (average cold wall), q, Btu/ft^2-sec	Total heat load (cold wall), Q, Btu/ft^2
				Exposure time		Termination of exposure			Maximum temperature rise		Total back-surface heat load		
Unit weight, w, lb/ft^2	Thickness, in.	Char-layer thickness, in.	Sublayer thickness, in.	t, sec for $\Delta T = 50^\circ$ F	t, sec for $\Delta T = 300^\circ$ F	t_f, sec	ΔT_f, $^\circ$F	$\left(\frac{dT}{dt}\right)_f$, $^\circ$F/sec	t_m, sec	ΔT_m, $^\circ$F	Q_B, Btu/ft^2-sec		
6.04	0.987	0.24	0.18	143	357	359	317	4.20	490	582	317	116	41,600
2.96	.473	.28	----	116	172	174	342	21.20	250	724	394	114	19,840
2.99	.476	.26	----	110	167	172	472	39.40	240	743	404	117	20,100
1.57	.248	.17	----	48	77	82	398	37.90	115	714	388	114	9,340
1.63	.261	.16	----	52	82	86	412	29.20	125	700	381	120	10,300
6.04	.987	.28	.53	185	---	173	46	.44	580	109	59	96	16,600
6.04	.987	.26	.52	196	---	190	49	.54	570	134	73	112	21,300
3.00	.479	.22	.16	119	---	120	52	2.20	254	245	133	92	11,000
1.50	.241	.12	.10	44	---	49	88	5.10	150	204	111	92	4,510

(b) Low-density phenolic nylon

3.00	0.925	0.204	-----	158	257	257	300	15.49	315	626	341	113	29,000
3.00	.927	.188	-----	140	256	258	340	26.00	310	703	382	96	24,800
1.50	.476	.165	-----	85	115	119	495	43.10	140	711	387	93	11,070
1.50	.450	.167	-----	92	120	125	459	36.0	150	637	347	114	14,250
3.00	.930	.148	0.181	112	---	210	215	2.60	285	344	187	112	23,500
3.00	.934	.140	.440	130	---	130	50	7.90	190	134	73	97	12,600
3.00	.933	.134	.480	123	---	129	59	3.65	280	155	84	105	13,600
1.50	.417	.163	.093	89	---	93	64	4.70	170	220	120	94	8,740

2 in 65

20

"The aeronautical and space activities of the United States shall be conducted so as to contribute . . . to the expansion of human knowledge of phenomena in the atmosphere and space. The Administration shall provide for the widest practicable and appropriate dissemination of information concerning its activities and the results thereof."

—NATIONAL AERONAUTICS AND SPACE ACT OF 1958

NASA SCIENTIFIC AND TECHNICAL PUBLICATIONS

TECHNICAL REPORTS: Scientific and technical information considered important, complete, and a lasting contribution to existing knowledge.

TECHNICAL NOTES: Information less broad in scope but nevertheless of importance as a contribution to existing knowledge.

TECHNICAL MEMORANDUMS: Information receiving limited distribution because of preliminary data, security classification, or other reasons.

CONTRACTOR REPORTS: Technical information generated in connection with a NASA contract or grant and released under NASA auspices.

TECHNICAL TRANSLATIONS: Information published in a foreign language considered to merit NASA distribution in English.

TECHNICAL REPRINTS: Information derived from NASA activities and initially published in the form of journal articles.

SPECIAL PUBLICATIONS: Information derived from or of value to NASA activities but not necessarily reporting the results of individual NASA-programmed scientific efforts. Publications include conference proceedings, monographs, data compilations, handbooks, sourcebooks, and special bibliographies.

Details on the availability of these publications may be obtained from:

SCIENTIFIC AND TECHNICAL INFORMATION DIVISION

NATIONAL AERONAUTICS AND SPACE ADMINISTRATION

Washington, D.C. 20546